

Manuscript Number: AB-18-2613R2

Title: A Soft 3D Polyacrylate Hydrogel Recapitulates the Cartilage Niche and Allows Growth-factor Free Tissue Engineering of Human Articular Cartilage

Article Type: Full length article

Keywords: Polyacrylate; poly(methylmethacrylate-co-methacrylic acid); Polymer microarray; hydrogel; cartilage tissue engineering

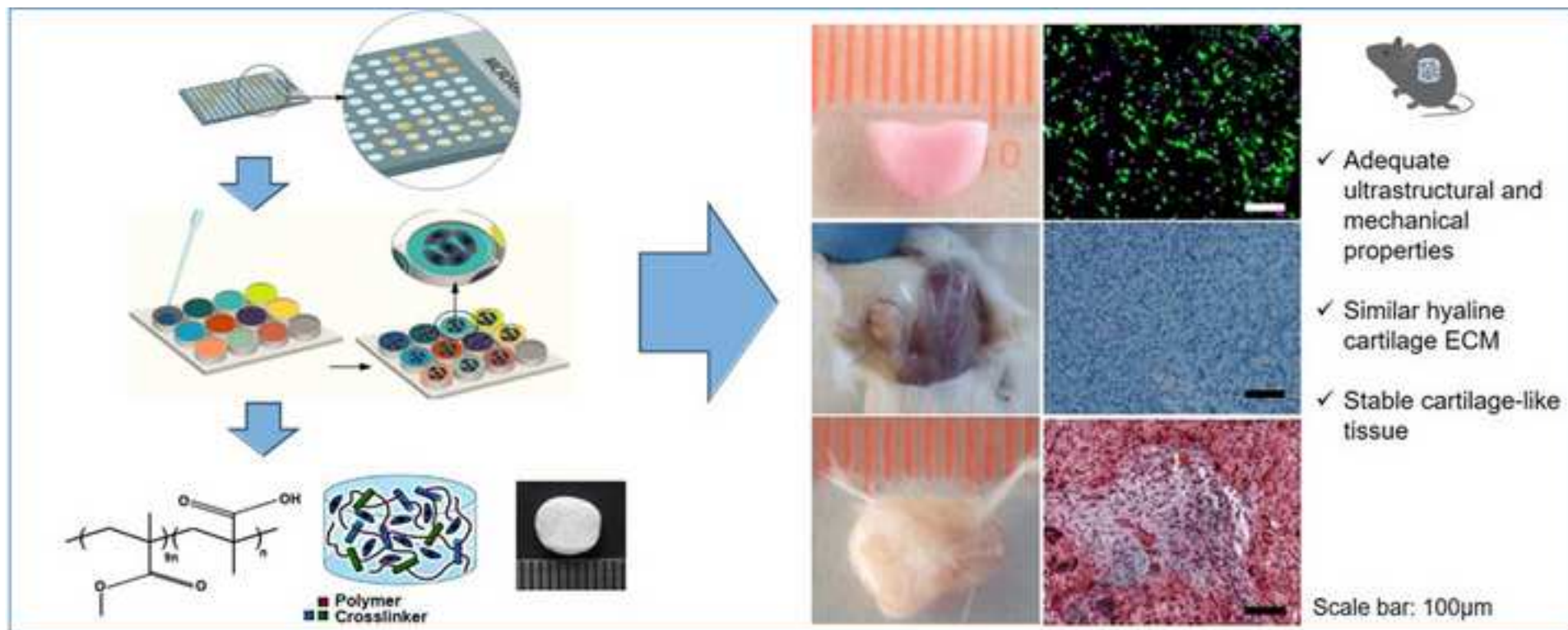
Corresponding Author: Professor Juan Antonio Marchal, M.D., Ph.D.

Corresponding Author's Institution: University of Granada

First Author: Gema Jiménez, Dr

Order of Authors: Gema Jiménez, Dr; Seshasailam Venkateswaran, Dr; Elena López-Ruiz, Dr; Macarena Perán, Dr; Salvatore Pernagallo, Dr; Juan J. Díaz-Monchón, Dr; Raphael F. Canadas, Dr; Cristina Antich; Joaquín M. Oliveira, Dr; Anthony Callanan, Dr; Robert Walllance, Dr; Rui L. Reis, Prof.; Elvira Montañez, Dr; Esmeralda Carrillo, Dr; Mark Bradley, Prof.; Juan Antonio Marchal, M.D., Ph.D.

Abstract: Cartilage degeneration or damage treatment is still a challenge, but, tissue engineering strategies, which combine cell therapy strategies, which combine cell therapy and scaffolds, and have emerged as a promising new approach. In this regard, polyurethanes and polyacrylates polymers have been shown to have clinical potential to treat osteochondral injuries. Here, we have used polymer microarrays technology to screen 380 different polyurethanes and polyacrylates polymers. The top polymers with potential to maintain chondrocyte viability were selected, with scale-up studies performed to evaluate their ability to support chondrocyte proliferation during long-term culture, while maintaining their characteristic phenotype. Among the selected polymers, poly(methylmethacrylate-co-methacrylic acid), showed the highest level of chondrogenic potential and was used to create a 3D hydrogel. Ultrastructural morphology, microstructure and mechanical testing of this novel hydrogel revealed robust characteristics to support chondrocyte growth. Furthermore, in vitro and in vivo biological assays demonstrated that chondrocytes cultured on the hydrogel had the capacity to produce extracellular matrix similar to hyaline cartilage, as shown by t increased expression of collagen type II, aggrecan and Sox9, and the reduced expression of the fibrotic marker's collagen type I. In conclusion, hydrogels generated from poly(methylmethacrylate-co-methacrylic acid) created the appropriate niche for chondrocyte growth and phenotype maintenance and might be an optimal candidate for cartilage tissue-engineering applications.



1 **A Soft 3D Polyacrylate Hydrogel Recapitulates the Cartilage Niche and Allows Growth-factor**
2 **Free Tissue Engineering of Human Articular Cartilage**

3
4
5
6
7
8
9
10
11
12
13
14
15
16
17
18
19
20
21
22
23
24
25
26
27
28
29
30
31
32
33
34
35
36
37
38
39
40
41
42
43
44
45
46
47
48
49
50
51
52
53
54
55
56
57
58
59
60
61
62
63
64
65

Gema Jiménez^{1,2,3,4,†}, Seshasailam Venkateswaran^{5,†}, Elena López-Ruiz^{1,3,4,6,†}, Macarena Perán^{1,4,6},
Salvatore Pernagallo⁷, Juan J. Díaz-Monchón^{8,9}, Raphael F. Canadas^{10,11}, Cristina Antich^{1,2,3,4},
Joaquím M. Oliveira^{10,11,12}, Anthony Callanan¹³, Robert Wallace¹⁴, Rui L. Reis^{10,11,12}, Elvira
Montañez¹⁵, Esmeralda Carrillo^{1,2,3,4}, Mark Bradley^{5,*} and Juan A. Marchal^{1,2,3,4,*}

¹ Biopathology and Regenerative Medicine Institute, Centre for Biomedical Research, University of
Granada, 18100 Granada, Spain.

² ~~Biosanitary Research Institute of Granada~~ Instituto de Investigación Biosanitaria ibs.GRANADA,
Universidad de Granada, 18100 Granada, Spain

³ Department of Human Anatomy and Embryology, Faculty of Medicine, University of Granada,
18016 Granada, Spain.

⁴ Excellence Research Unit “Modeling Nature” (MNat), University of Granada, Spain

⁵ School of Chemistry, EaStCHEM, University of Edinburgh, King's Buildings, West Mains Road,
Edinburgh, EH9 3JJ, UK.

⁶ Department of Health Sciences, University of Jaén, Jaén E-23071, Spain.

⁷ DestiNAGenómica S.L. Parque Tecnológico Ciencias de la Salud, Avenida de la Innovación 1,
Edificio Business Innovation centre, 18016 Granada, Spain.

⁸ Pfizer-Universidad de Granada-Junta de Andalucía Centre for Genomics and Oncological
Research (GENYO), Parque Tecnológico de Ciencias de la Salud, 18016 Granada, Spain.

⁹ Faculty of Pharmacy, University of Granada, 18071 Granada, Spain

¹⁰ 3Bs Research Group, Biomaterials, Biodegradables and Biomimetics, University of Minho,
Headquarters of the European Institute of Excellence on Tissue Engineering and Regenerative
Medicine, AvePark, 4805-017 Barco, Guimarães, Portugal.

¹¹ ICVS/3Bs, PT Government Associate Laboratory, Braga, Guimarães, Portugal.

28 ¹² The Discoveries Centre for Regenerative and Precision Medicine, Headquarters at University of
129 Minho, Avepark, 4805-017 Barco, Guimarães, Portugal.

2
3
4
5
6
7
8
9
10
11
12
13
14
15
16
17
18
19
20
21
22
23
24
25
26
27
28
29
30
31
32
33
34
35
36
37
38
39
40
41
42
43
44
45
46
47
48
49
50
51
52
53
54
55
56
57
58
59
60
61
62
63
64
65

¹³ Institute for Bioengineering, School of Engineering, University of Edinburgh, EH93JL
Edinburgh, UK

¹⁴ Department of Orthopaedics, The University of Edinburgh, EH16 4SB Edinburgh, UK

¹⁵ Department of Orthopedic Surgery and Traumatology, Virgen de la Victoria University Hospital,
29010 Málaga, Spain.

†These authors contributed equally to this work.

* Corresponding authors.

54 **Abstract**

1
255 Cartilage degeneration or damage treatment is still a challenge, but, tissue engineering strategies,
3
456 which combine cell therapy strategies, which combine cell therapy and scaffolds, and have emerged
5
6
757 as a promising new approach. In this regard, polyurethanes and polyacrylates polymers have been
8
958 shown to have clinical potential to treat osteochondral injuries. Here, we have used polymer
10
11
1259 microarrays technology to screen 380 different polyurethanes and polyacrylates polymers. The top
13
1460 polymers with potential to maintain chondrocyte viability were selected, with scale-up studies
15
16
1761 performed to evaluate their ability to support chondrocyte proliferation ~~in~~ during long-term culture,
18
1962 while maintaining their characteristic phenotype. Among the selected polymers,
20
2163 poly(methylmethacrylate-co-methacrylic acid), showed the highest level of chondrogenic potential
22
23
2464 and was used to create a 3D hydrogel. Ultrastructural morphology, microstructure and mechanical
25
2665 testing of this novel hydrogel revealed robust characteristics to support chondrocyte growth.
27
28
2966 Furthermore, *in vitro* and *in vivo* biological assays demonstrated that chondrocytes cultured on the
30
3167 hydrogel had the capacity to produce extracellular matrix similar to hyaline cartilage, as shown by
32
33
3468 increased expression of collagen type II, aggrecan and Sox9, and the reduced expression of the
35
3669 fibrotic marker's collagen type I. In conclusion, hydrogels generated from
37
38
3970 poly(methylmethacrylate-co-methacrylic acid) created the appropriate niche for chondrocyte growth
40
4171 and phenotype maintenance and might be an optimal candidate for cartilage tissue-engineering
42
4372 applications.

44
45
46
4773
48
49
5074 **Keywords:** Polyacrylate; poly(methylmethacrylate-co-methacrylic acid); Polymer microarray;
51
5275 hydrogel; cartilage tissue engineering
53
54
55
5676
57
58
5977
60
61
62
63
64
65

78 **1. Introduction**

1
279 Hyaline cartilage is subjected to high degrees of wear that is exacerbated by its avascular nature,
3
480 which limits its regeneration. Its degradation is debilitating to athletes, the elderly and patients
5
6
781 suffering from pathologies such as osteoarthritis, leading to severe pain and loss of mobility [1]. In
8
982 clinical scenarios, autologous chondrocyte implantation is a preferred strategy for repairing articular
10
11
1283 cartilage damage. However, harvesting of chondrocytes is restricted to small, non-load-bearing
13
1484 areas of the cartilage leading to low yields of cells [2] thus chondrocytes have to be expanded *in*
15
1685 *vitro* prior to implantation. Nevertheless, during traditional 2D culture these cells lose their
17
18
1986 phenotype and become hypertrophic [3]. This is in part due to the fact that the extracellular matrix
20
2187 (ECM) produced by the cells cultured in monolayers lacks the functional cues and characteristics of
22
23
2488 native cartilage tissue [4]. Interestingly, chondrocytes proliferate and retain their phenotype in 3D
25
2689 culture systems producing cartilage-like ECM [5, 6]. Hence, treatment of cartilage lesions is
27
28
2990 currently based on bioabsorbable 3D matrices [7] of porcine collagen type I and III or hyaluronic
30
3191 acid, which are used to culture autologous chondrocytes *in vitro*, for subsequent implantation of the
32
33
3492 cell-laden scaffold. Yet, the clinical outcomes of scaffold-assisted approaches have been shown to
35
3693 be similar to those of scaffold-free autologous chondrocyte implantation [8, 9]. This technique also
37
38
3994 suffers from the disadvantage of applying animal-derived collagen scaffolds with the possibility of
40
4195 adverse immune reactions.

42
43
4496 Bioabsorbable synthetic polymers such as poly(lactic acid), poly(glycolic acid) and
45
46
4797 polycaprolactone have been explored [10,11,12]. Synthetic biodegradable polymers, like their
48
4998 natural-origin counterparts such as collagen and hyaluronic acid, display markedly different rates of
50
5199 scaffold degradation/remodelling compared to that of the ECM [13]. Hence, slow-bioabsorbable but
52
53
5400 biocompatible scaffolds allowing cell attachment, proliferation, and triggering the synthesis of
55
56
5701 appropriate ECM for efficient *in vivo* tissue regeneration, would be a major advance. In this regard,
58
5902 polyurethanes and polyacrylates have been shown to have clinical potential to treat osteochondral
60
6103 lesions [14, 15]. Polyurethanes have been employed to reproduce both soft and hard tissues [16],
62
63
64
65

104 including cartilage, while polyacrylates have been shown to induce chondrogenesis of mesenchymal
105 stem cells even in the absence of chondrogenic induction factors [14]. Hydrogels represent a good
106 choice as 3D matrices to support chondrocytes and treat cartilage lesions, because these systems can
107 be engineered to exhibit similar mechanical, swelling, and lubricating behaviour as articular
108 cartilage [17]. Moreover, hydrogels can be adapted to the defect shape, and deliver cells for lesion
109 regeneration more efficiently than scaffold-free techniques [18], while the use of ester-based cross-
110 linkers would allow slow degradation.

111 In this work, we aimed to identify and develop novel hydrogel polymers with chondrogenic cell
112 binding and proliferation properties for tissue engineering applications. Polymer microarrays
113 [19,20,21] were used to parallel screen hundreds of polymers to identify poly(methylmethacrylate-
114 *co*-methacrylic acid) (PA204) as a potential substrate for adhesion and proliferation of primary
115 human chondrocytes for use in cartilage tissue engineering. From this lead material, highly porous
116 3D matrices were fabricated by crosslinking the monomers of PA204 with poly(ethyleneglycol)
117 diacrylate (PEGDA) using a combination of water and polyethyleneglycol (PEG) as porogens.
118 Extensive analyses of the ECM produced in these gels were conducted as were *in vivo* integration in
119 a mouse model.

120 121 **2. Materials and methods**

122 **2.1. Isolation and culture of human articular chondrocytes**

123 Articular cartilage obtained from patients with knee osteoarthritis (described in detail in
124 Supplementary data) was minced and digested overnight in 0.08% collagenase IV (Sigma) digestion
125 at 37°C with gentle agitation. Cells were centrifuged and rinsed with buffer to remove the
126 collagenase. The remaining cells were then plated in flasks and cultured in chondrocytes medium:
127 DMEM (Sigma) supplemented with 20% fetal bovine serum (FBS, Gibco), 5 ml of 1% ITS
128 (Insulin-Transferrin-Selenium, Gibco), 100 U/ml penicillin and 100 µg/ml streptomycin at 37°C in
129 a humidified atmosphere of 5% CO₂. After 24 hours medium was replaced with fresh medium

130 supplemented with 10% FBS. At 80% of confluency cells were detached with TrypLE (Invitrogen)
131 and sub-cultured.

2
3
132
4

133 **2.2. Polymer microarray**

7
134 *a. Preparation:* The polymer library used was prepared on gram-scale by parallel synthesis, and all
9 individual members were fully characterised by gel permeation chromatography (GPC), differential
10 scanning calorimetry (DSC) and contact angle measurements [22]. Three hundred and eighty
11 members of a pre-synthesised polyurethane (PU) and polyacrylate/acrylamide (PA) library were
12 “spotted” onto aminoalkylsilane-treated glass slides, previously coated with agarose to prevent
13 non-specific cell adhesion [23]. Before printing in a microarray-type format each library member
14 was dissolved in a common, non-volatile solvent 1-methyl-2-pyrrolidinone (NMP). Coating with
15 agarose was achieved by manually dip-coating the slide in agarose Type I-B (1% w/v in deionised
16 water at 65°C), followed by removal of the coating on the bottom of the slide by wiping with a clean
17 piece of tissue. Subsequently, slides were dried overnight at room temperature in a dust-free
18 environment. Polymers for contact printing were prepared by dissolving 10 mg of polymer in 1 ml
19 of the non-volatile solvent N-methyl-2-pyrrolidinone. Polymer microarrays were then fabricated by
20 contact printing (Q-Array Mini microarrayer) with 32 aQu solid pins (K2785, Genetix) using the
21 polymer solutions placed in polypropylene 384-well microplates (X7020, Genetix). The 380
22 members of the polymer libraries were printed following a four-replicate pattern with 1 single field
23 of 32×48 spots containing 4 control (emptied) areas. Printing conditions were as follows: 5
24 stampings per spot, 200 ms sinking time, and 10 ms stamping time. The typical spot size was 300–
25 320 µm diameter with a pitch distance of 560 µm (y-axis) and 750 µm (x-axis), allowing up to 1520
26 features to be printed on a standard 25×75 mm slide. Once printed, the slides were dried under
27 vacuum (12 h at 42 °C/200 mbar) and sterilised in a bio-safety cabinet by exposure to UV
28 irradiation for 20 min prior to use.

29
135
30
31
32
136
33
34
137
35
36
138
37
38
139
39
40
41
42
140
43
44
141
45
46
142
47
48
143
49
50
144
51
52
145
53
54
55
56
57
58
59
146
60
61
62
63
64
65

156 *b. Cell culture:* For polymer library screening, suspensions of cell populations in 5 ml of media
157 were plated (3×10^5 cells/well) onto two identical polymer microarrays containing 380 polymers
158 (PUs and PAs). Articular chondrocytes were grown in DMEM–high glucose (Sigma) supplemented
159 with 10% FBS (Sigma), 1% penicillin-streptomycin (Sigma) and 1% ITS (Gibco).

161 **2.3. Polymer coating of well plates**

162 *a. Preparation:* For large-scale analysis, polymer coating of 12 well plates were prepared by
163 incubating 250 μ L of each polymer solutions (2.0% w/v in acetic acid) for 30 min at 4°C under
164 gentle shaking and left to air-dry overnight in the hood at room temperature. The coated wells were
165 then irradiated with ultraviolet (UV) light for 30 min and washed with PBS two times (5 min per
166 wash) prior to cellular studies.

167 *b. Cell culture:* For large-scale analysis of the hit polymers (see Table S2), cells were seeded at
168 3×10^4 cells per well of the polymer-coated 12 well plate. After 10 days in culture, cells were fixed
169 with 4% paraformaldehyde for 20 min and stained with toluidine blue and alizarin red as previously
170 described [24].

172 **2.4. Hydrogels**

173 *a. Preparation:* Combinations of the monomers that made up PA204 (90% Methyl methacrylate
174 (MMA) and 10% Methacrylic acid (MA-H) were dissolved in 1-methyl-2-pyrrolidinone (NMP) and
175 a solution of tetramethylethylene diamine (TEMED). Poly(Ethylene Glycol) Diacrylate (PEGDA)
176 (MW = 700 Da) and Poly(Ethylene Glycol) (PEG) (MW = 3000 Da) were added sequentially (see
177 Table 2). Solutions were mixed for 1 min, and polymer hydrogel synthesis was achieved, in syringe
178 barrels, by adding the redox initiator (ammonium persulfate (APS)). The reaction mixture was kept
179 at 37 °C overnight. Hydrogels were washed with ethanol three times (30 min) and with PBS four
180 times to remove unreacted material (3x30 min and 1xovernight washes) and stored in water at RT.
181 In order to obtain lyophilised scaffolds, hydrogels were frozen on dry ice for 5 min, transferred to a

182 -80°C freezer overnight and, then, freeze-dried at 1 mbar and -45°C. Non-lyophilised and
183 lyophilised hydrogels were cut into 2 mm discs, and were sterilised with 70% (v/v) ethanol 30 min
2
3
184 and, then, rinsed three times in PBS, and finally were treated with UV light for 15 min.
4
5
6
185

8
186 *b. Cell culture:* Hydrogel (2 mm thick disks) were placed overnight in medium and an aliquot of
10
11
187 suspended chondrocytes (2×10^5 cells/100 μ L) pipetted onto each specimen and incubated for 4 h at
12
13
188 37°C to allow cell attachment. The cell-seeded scaffolds were transferred into new 24-well culture
15
16
189 plates with 1 mL of medium. All samples were incubated under a 5% CO₂ atmosphere at 37°C for
17
18
190 48 hours or 21 days. The culture medium was replaced every 2 days and the hydrogels were
20
21
191 processed (as above) for subsequent analysis.
22
23
24
25

26 **2.5. Micro-CT analysis**

27
28
194 The scanning of the scaffolds was conducted under 50 keV and 200 μ A in a micro-CT (1272
29
30
195 scanner; SkyScan, Kontich, Belgium). The integration time ranged from 0.4 to 0.6 s, the rotation
32
33
196 step was 0.1° over a total rotation of 360°. The acquired image pixel resolution ranged from 3.0 to
34
35
197 4.5 μ m. Qualitative visualization of the morphology was performed using the CTvox software
37
38
198 (Skyscan). The porosity, open porosity, pore size and trabecular thickness were processed in
39
40
199 standardized software (CT Analyser, version 1.15.4.0, Skyscan). 3 specimens were used for the
42
43
200 quantitative microstructure evaluation.
44
45
46
47

48 **2.6. Mechanical characterization**

49
50
203 Hydrogels with a diameter of 9.5 mm and a height of 8.5 and 6.7 mm for non-lyophilized and
51
52
204 lyophilized, respectively, were used for mechanical test. The diameter of the scaffolds was
54
55
205 measured using a digital Vernier Caliper. Stiffness of the samples was measured using a stress-
56
57
206 controlled rheometer (DHR-2, TA Instruments). Axial compression tests (37 °C) were performed at
59
60
207 constant speed (10 micrometers/s) using a sandblasted plate-plate geometry (diameter 40 mm) to
61
62
63
64
65

208 minimize wall slip and normal force (N), stress (N/m²) and strain were determined. The stiffness of
209 the scaffolds (at 0-5%, 0-10% and 0-15% strain) was measured by determining the slope of the plot
210 of stress vs strain.

212 **2.7. Biological characterization**

213 Viability assay, histological and immunohistochemical analysis, real time-PCR analysis,
214 GAGs/DNA content, and alamar blue assay are described in detail in the Supplementary data
215 section.

217 **2.8. *In vivo* assays**

218 *In vivo* experiments were performed in immunocompetent CD-1 and immunodeficient NOD SCID
219 (NOD.CB17-Prkdcscid/NcrCrl) (NSG) purchased from Charles River (Barcelona, Spain). In order
220 to evaluate the biocompatibility, control hydrogels without cells were transplanted into the back
221 subcutaneous tissue of CD-1 mice anesthetized (n=6) by isoflurane inhalation. Also, hydrogels were
222 cultured with cells during 21 days and, then, transplanted into the back subcutaneous tissue of NSG
223 mice anesthetized (n=6) by isoflurane inhalation. Animals were maintained in a microventilated
224 cage system with a 12-h light/dark cycle with food and water *ad libitum*. Mice were manipulated
225 within a laminar air-flow to maintain pathogen-free conditions. Three weeks later (CD-1) or four
226 weeks later (NSG), mice were sacrificed *via* an overdose injection of anaesthetic, and pellets with
227 new tissue formed around them were excised for further analysis. *In vivo* assays were carried out in
228 accordance with the approved guidelines of University of Granada following institutional and
229 international standards for animal welfare and experimental procedure. All experimental protocols
230 were approved by the Research Ethics Committee of the University of Granada.

234 **2.9. Statistics analysis**

235 All graphed data represent the mean +/-SD from at least three experiments. Differences between
2 treatments were tested using the two-tailed Student's T test. Assumptions of Student's T test
236 (homocedasticity and normality) were tested and assured by using transformed data sets
237 [log(dependent variable value +1)] when necessary. P-values <0.01 (**, ##) and <0.05 (*, #,) were
238 considered statistically significant in all cases.
239

241 **3. Results and discussion**

242 **3.1. Polymer microarray screening and polymer-coated plates demonstrate the potential for** 243 **chondrocytes culture polyacrylate and polyurethane polymers**

244 Freshly isolated chondrocytes were seeded onto a polymer microarray (containing 1536 features,
245 i.e., 380 polymers and 4 controls each in quadruplicate). After 72 hours of culture, adhesion of
246 chondrocytes to the polymers was evaluated by counting the average number of DAPI-stained
247 nuclei on each feature. Viability of the cells on the microarrays was confirmed with CellTracker™
248 green (CTG) for subsequent scale-up and, hence, the biocompatibility of the polymers (Figure S1).
249 Ten polymers (Tables 1 and S2) were selected in terms of efficiency of cell binding and solubility
250 in the solvent acetic acid (required to enable coating the polymer onto polystyrene well plates).
251 Scale-up studies were performed to evaluate their ability to support the chondrocyte phenotype, cell
252 proliferation and long-term culture. Thus, well plates were coated with selected polymers (2.0% w/v
253 in acetic acid) and chondrocytes were cultured (2, 4, 7 and 10 days), stained with toluidine blue or
254 alizarin red and analysed by phase-contrast light microscopy (Figure S2). Toluidine blue staining
255 (to determine the presence of glycosaminoglycans (GAGs) [3]) was low on PU153, PA202 and
256 PA309, while PA167 did not allow cell attachment and the number of cells on PA460 was low.
257 Consequently, these polymers were excluded from further studies. Alizarin red staining, that stains
258 calcium deposits [24], revealed a potential osteoblast-like phenotype of cells growing on PA410
259 (Figure S2) and this polymer was also removed from further evaluation. The remaining 4 polymers

260 (PA204, PA234, PA391 and PA520) showed good cell attachment and maintenance of chondrocyte
261 phenotype, with PA204 providing the best performance (Figure S2).

262
263 Once the PA204 polymer was selected, a 3D experiment was performed in which a commercial
264 polycaprolactone (PCL) scaffold was coated with PA204 since scaffolds coated with polymers to
265 enhance chondrocyte adherence and proliferation have been shown previously [25, 26]. Here, we
266 used PA204 (2.0% w/v in acetic acid) to coat the surface of the commercial PCL scaffolds, the
267 "gold standard" in cartilage tissue engineering [28]. Analysis to test chondrocytes culture viability
268 on the coated surfaces were performed and results showed a the coating to be non-cytotoxic and
269 demonstrated increased cell proliferation (Figure S3a). Others have shown that the coating of PCL
270 scaffolds improves the composition of secreted ECM [29]. In our study, collagen type II expression
271 was similar in coated and non-coated PCL scaffolds, while environmental scanning electron
272 microscope (ESEM) images evidenced a dense ECM secretion that covered the surface, with a
273 good adhesion and homogenous distribution of chondrocytes throughout the entire scaffold (Figure
274 3Sb-c).

275 276 **3.2. Generation and biological validation of poly(methylmethacrylate-co-methacrylic acid)** 277 **(PA204) hydrogels by combination of porogens and a biocompatible cross-linkers.**

278 Based on polymer microarray and polymer-coated well plate results the polymer PA204 was
279 processed into hydrogels by incorporating a hydrophilic and biocompatible cross-linker PEG-
280 diacrylate (PEGDA, 700 Da) and porogens in order to generate gels with an optimal porous
281 structure [30]. Initially, cylindrical gels of the polymer were produced in 2 mL syringes (using
282 ammonium persulphate/tetramethylethylenediamine as initiators) and gave gels, which although
283 offering robust handling were translucent indicating a poorly porous structure. Hydrogels should
284 have an optimal porous structure to allow the diffusion of nutrients and waste products [31].
285 However, this fact is inversely related with the mechanical properties of the hydrogels [32] and led

286 to the generation of a series of gels that combined a porogen (PEG, 3 kDa) and a ‘poor solvent’
287 (water), to induce precipitation during polymerisation to give hydrogels with a more porous
288 structure [33]. PEG as a porogen is used to form biocompatible hydrogels with a three-dimensional
289 structure [34] and PEG of ~ 3 kDa can provide a narrow pore size distribution and offers good
290 morphological and mechanical characteristics to the hydrogels [35]. It enhances diffusion of
291 macromolecules into the interior of polyacrylamide and PEG hydrogel after the polymerization by
292 creating microfluidic channels [36]. The numbers and size of microfluidic channels (representing
293 the porosity) can be controlled by several methods, including the use of increasing concentrations of
294 porogens [37]. PA204 based gels lacked large pores until the PEG porogen and water content of the
295 polymerisation solutions was increased to >2% and >20% respectively. Although both the water
296 and porogen levels were increased simultaneously, the water content had a more profound effect on
297 inducing porosity. ESEM images revealed that in the absence of precipitation (and hence the
298 globular, interconnected structure) induced by the poor solvent, the polymers were not porous.
299 When the water content of the polymerisation solution was increased from 15% to 20% a porous
300 matrix was obtained (data not shown). PA204 based gels offered the capacity to contain more water
301 (~95%), perhaps due to the presence of the hydrophilic methacrylic acid monomer units (Table 2).
302 In addition, lyophilisation was used to increase the porosity of the novel PA204 hydrogels. In fact,
303 this method has been used before for the fabrication of porous hydrogels for tissue engineering [38].
304
305 Biological characterisation of two hydrogel variants of PA204 (PA204-2 and PA204-2A) (Table 2)
306 was performed to assess their ability to support chondrocyte viability and phenotype. Both PA204
307 based gels were able to maintain cell viability of freshly isolated human chondrocytes and cultured
308 for 21 days between 98 and 99%, with the exception of PA204-2A lyophilised hydrogel which was
309 approximately 60% (Figure S4). Cell morphology varied depending on the different matrices, with
310 cells seeded on PA204-2 lyophilised versions having an ellipsoidal shape, which is typical of
311 chondrocytes in the superficial regions of cartilage (Figure 1a and Figure S4) [39].

312 Immunofluorescence analysis on lyophilised and non-lyophilised gels showed that the PA204-2
313 hydrogel was able to promote the formation of a cartilage tissue-like ECM with higher expression
2 of
314 of collagen type II, a characteristic marker of mature chondrocyte phenotype, and without
4
5
315 expression of collagen type I (fibrotic marker) (Figure 1b) [40]. Moreover, histological analysis
7
316 confirmed the presence of cartilage-specific ECM components produced by chondrocytes. Efficient
9
10
317 penetration of cells (pink cytoplasm) was found in all the hydrogels, while blue staining of
12
1318 proteoglycans was more abundant for the lyophilised gels (Figure 1c). Overall, greater levels of
14
15
319 cartilage specific ECM components were secreted on the PA204-2 based gels: the acidic dye in the
16
17
1820 Masson-trichrome staining showed more collagen fibers (green) and the basic dye, Alcian blue
19
20
321 showed more proteoglycan. The biological characterization showed that PA204-2 showed better
21
22
2322 results compared to PA204-2A and so was used for all further studies.
24

25
26

3.3. Ultrastructural and mechanical characterization showed that lyophilisation of PA204-2 hydrogel improved physical parameters such as porosity and interconnectivity.

327 Based on the previous results, the PA204-2 polymer (Figure 2a) was processed into 3D hydrogels
34
3527 with rounded shape with a size of 7mm x 3mm (W x H) (Figure 2b). Ultra-morphology and
36
37
328 microstructure of the PA204-2 hydrogel were studied by ESEM and X-ray micro-computed
38
39
4029 tomography (micro-CT) respectively (Figure 2c-d). Ultra-morphology gave a microstructure
41
42
330 interconnected to form a dense fibrillar structure. The hydrogel had a homogenous microporous
43
44
4531 system in which the pore diameters—varied among both the non-lyophilised (20 μm) and the
46
47
332 lyophilised materials (50 μm) and were interconnected to form a macroporous structure (Figure 2c-
48
49
333 d). It was found that the percentage of porosity for lyophilised hydrogels was close to 91% with
51
52
334 highly interconnected pores (91% of open porosity) with the pore size about 51 μm (in concordance
53
54
335 with the ESEM observations), and the trabecular thickness 15 μm . In contrast the non-lyophilised
55
56
336 hydrogels showed significant differences, with reduced porosity (81%) and interconnectivity (81%),
58
59
337 as well as smaller pore sizes (21 μm) and trabecular thickness (9 μm) (Figure 2e). Thus our results
60
61
62
63
64
65

338 showed that lyophilisation process induced higher porosity and larger pore size as previously shown
339 by others [38]. Although, it was reported that high porosity and interconnectivity (80-90%) support
2 effective nutrient supply, gas diffusion and metabolic waste removal for cartilage regeneration [41],
340 3
4
5
341 there is still controversy regarding the appropriate porosity and pore size. Others studies have
7
342 proposed that hydrogels should have a porosity as high as 90% to facilitate cell attachment,
9
10
343 proliferation and matrix deposition [39, 40], and a small mean pore size ranged from 20-150 μm to
12
13
344 enhance the deposition of a hyaline-like ECM and, thus, neo-cartilage formation [41,42].
14
15
345 Additionally, as expected, the stiffness decreased with increasing porogen and water content. The
16
17
346 stiffness of lyophilised hydrogels was 14 kPa when a strain between 10-15% was applied ($p < 0.01$),
19
20
347 very similar to the non-lyophilised materials that were closer to 10 kPa when subjected to the same
21
22
348 strain (Figure 3f). The stiffness of both hydrogels are thus appropriate to maintain the homeostatic
24
25
349 balance between catabolism and anabolism in chondrocytes [46]. The stiffness of these hydrogels
26
27
350 was compared after 8 weeks storage in water, to determine how changes in stiffness over time
29
30
351 would affect the behaviour of chondrocytes, however, both gels showed no change after 8 weeks
31
32
352 (data not shown).

353 36 37 354 **3.4. Biological characterization revealed that PA204-2 lyophilised hydrogel supported long-** 38 39 40 355 **term chondrocytes culture and the production of an ECM similar to the native cartilage**

41
42
356 ESEM revealed that the chondrocytes attached to both lyophilised and non-lyophilised PA204-2
43
44
45 based hydrogels (after 21 days' culture) actively produced ECM components resulting in a dense
46
47
358 matrix that covered the interconnected globules of the gels (Figure 43a). Gene expression analysis
48
49
359 showed elevated expression of chondrocyte markers (collagen type II and Sox9) [43,44,45] with
51
52
360 reduced expression of the markers for the fibroblastic phenotype (collagen type I) [49] on the
53
54
361 lyophilised gels when compared to the non-lyophilised gels and the 2D (*p-value) and 3D controls
55
56
362 (#p-value) (Figure 3b). GAGs produced by cultured chondrocytes were solubilized by proteolytic
58
59
363 digestion and quantified by the 1,9-Dimethylmethylene Blue colorimetric method. Both
60
61
62
63
64
65

364 hydrogels showed an increase in the deposition of GAGs after 21 days of culturing, however, the
365 final amount was significantly higher in the PA204-2 lyophilised hydrogel. This fact indicates that
2
366 the lyophilised hydrogel was advantageous for supporting the maintenance of a mature chondrocyte
4
5
367 phenotype (Figure 4c), showing an ECM similar to native cartilage, composed by high amount of
7
368 GAGs [40].
9

10
1369
12
1370 An adequate proliferative capacity and metabolic activity are necessary to obtain a suitable tissue
14
15
1371 substitute [50], with these characteristics reducing the level of chondrocyte senescence [51]. In
16
17
1372 order to quantify the adhesion and proliferation of chondrocytes an Alamar blue assay was
19
20
1373 performed. Results demonstrated that chondrocyte proliferation was constant and similar in both
21
22
1374 hydrogels, with a significant increase in cell number throughout 21 days of culture (Figure 3d), as
24
25
1375 described previously [52]. Therefore, the process of lyophilisation did not affect either cell
26
27
1376 attachment or proliferation.
29

30
31
32
1377
33
34
35
36
37
380 **3.5. *In vivo* assay demonstrated high biocompatibility of both PA204-2 lyophilised and non-
39
40
41
42
43
44
45
46
47
48
49
50
51
52
53
54
55
56
57
58
59
60
61
62
63
64
65**
381 **lyophilised hydrogels, but chondrocytes cultured in lyophilised hydrogels showed enhanced
382
383
384
385
386
387
388
389
390
391
392
393
394
395
396
397
398
399
400
401
402
403
404
405
406
407
408
409
410
411
412
413
414
415
416
417
418
419
420
421
422
423
424
425
426
427
428
429
430
431
432
433
434
435
436
437
438
439
440
441
442
443
444
445
446
447
448
449
450
451
452
453
454
455
456
457
458
459
460
461
462
463
464
465**
466 **expression of chondrogenic markers.**

467 Finally, the biocompatibility of the lyophilised and non-lyophilised hydrogels was assessed *in vivo*
468 in a mouse model. First, with the aim to analyse polymer compatibility, hydrogels without cells
469 were transplanted into subcutaneous tissue on the flanks of immunocompetent mice CD-1. Three
470 weeks later, hydrogels were harvested and showed an adequate integration in the subcutaneous
471 tissue with a layer of connective tissue adhered on the entire surface, maintaining their shape and
472 integrity, without any sign of oedema or inflammatory response to reject it (Figure 4a) [53]. In
473 addition, mice cells colonized the hydrogels deeply and showed a 100% viability (Figure 4b-c and
474 Figure S5a). Furthermore, histological analysis revealed ECM produced by the cells (Figure 4c),
475 that was more significant in lyophilized hydrogel.

390 Second, in order to evaluate cartilage-like characteristics *in vivo*, human freshly isolated
391 chondrocytes were cultured and encapsulated into the hydrogels (21 days), and then, cell-laden
392 hydrogels were transplanted into subcutaneous tissue on the flanks of immunodeficient NSG mice
393 and harvested 4 weeks later for subsequent analysis. The implanted cell-laden hydrogels were well
394 accepted by the mice and displayed a significant size increments and excellent cell viability. The
395 results demonstrated the biocompatibility and the integration of both lyophilised and non-
396 lyophilised PA204-2 hydrogels with the surrounding host tissue (Figure 5a) [54]. The implanted
397 cell-laden hydrogels were well accepted by the mice and displayed a significant size increments and
398 excellent cell viability (94% for non-lyophilised hydrogel and 99% for lyophilised hydrogel)
399 (Figure 5b and Figure S5b). In addition, ECM composition and chondrogenic mRNA expression
400 were evaluated to analyse if chondrocytes maintained their mature phenotype and secreted
401 characteristic hyaline matrix *in vivo*. Histological analysis showed a well-organized internal
402 structure with chondrocytes isolated in lacunas (H&E), and an ECM composed of collagen fibers
403 and proteoglycans, as revealed by Masson's trichrome and Alcian blue staining, respectively
404 (Figure 5b), all typical of native cartilage tissue [39]. Moreover, immunofluorescence staining with
405 mouse and human CD31 antibodies demonstrated that no blood vessels could be detected within the
406 hydrogels (Figure S6). Gene expression analysis confirmed increased expression for chondrogenic
407 markers, collagen type II and Sox9 ($p < 0.01$), on lyophilised hydrogels in comparison with non-
408 lyophilised hydrogels. Moreover, non-lyophilised hydrogels showed a 3-fold increase in the
409 expression of dedifferentiation-fibrotic marker collagen type I compared with lyophilised hydrogels
410 (Figure 5c) [55]. On the other hand, Acan mRNA expression was higher in non-lyophilised
411 hydrogels ($p < 0.05$), but quantification of GAGs levels was much higher on the lyophilised
412 hydrogels (Figure 5d). Definitely, both variants of PA204-2 hydrogel showed good *in vivo*
413 integration, although the lyophilised hydrogel proved to have a greater potential for the generation
414 of a tissue substitute more similar to the native cartilage tissue.

416 **4. Conclusion**

1
417 Polyacrylate based polymers that allow attachment and maintenance of chondrocytes were
3
418 identified using polymer microarray technology. Scale-up studies were performed to evaluate the
4
5
6
419 ability of ten hits polymers to support chondrocyte proliferation in long-term culture while
8
420 maintaining their characteristic phenotype. One of these polymers, PA204-2 showed better
10
11
421 biological and chemical characteristics and it was used to be synthesized as 3D matrices by the
12
13
422 preparation of cross-linked hydrogels using poly(methylmethacrylate-co-methacrylic acid),
14
15
423 poly(ethyleneglycol)diacrylate (as a crosslinker) and polyethyleneglycol (as a porogen). PA204-2
16
17
18
424 created the appropriate niche for chondrocyte growth and phenotype maintenance for long-term
20
21
425 culture and, when studied in a mouse model, supported the maintenance of a differentiated
22
23
426 chondrocyte phenotype, promoted cell proliferation and the secretion of a cartilage-like ECM.
25
427 Hence, the lyophilised PA204-2 hydrogel might be an optimal candidate for cartilage tissue
27
28
428 regeneration and can possibly overcome the limitations of the current scaffold-based approaches in
29
30
429 osteoarthritis treatment.
32

33
430
34

35 431 **Funding**

37
38
432 This work was supported by the Consejería de Economía, Innovación y Ciencia (Junta de
39
40
433 Andalucía, excellence project number CTS-6568) and by the Ministerio de Economía, Industria y
42
434 Competitividad (FEDER funds, project RTC-2016-5451-1). We acknowledge the Junta de
44
45
435 Andalucía for providing a fellowship granted to G.J. and the MINECO for providing a post-doctoral
47
436 fellowship to E.L-R (project RTC-2016-5451-1). MBR/SV thank the European Research Council
49
50
437 (Advanced Grant ADREEM ERC-2013-340469).
51

52 53 54 55 439 **Acknowledgments**

56
57
58
440 The authors also gratefully thank Ana Santos, Mohamed Tassi, Jose Manuel Entrena and Isabel
59
60
441 Sánchez from the C.I.C. (University of Granada) for excellent technical assistance, Tomás González
61
62
63
64
65

442 Justicia for his support with graphics and Elena Blanco from the University of Edinburgh for her
443 assistance with rheometer.

2
3
444
4
5

445 **Disclosures**

7
446 None of the authors have a conflict of interest to declare.

10
447
11
12

448 **References**

- 14
15
449 [1] D.M. Salter, (II) Cartilage, 31 (1998) 251–257.
16
17
450 [2] M. Brittberg, Autologous chondrocyte implantation--technique and long-term follow-up.,
19
20
451 Injury. 39 Suppl 1 (2008) S40-9.
21
22
452 [3] G. Jiménez, E. López-Ruiz, W. Kwiatkowski, E. Montañez, F. Arrebola, E. Carrillo, P.C.
24
25
453 Gray, J.C.I. Belmonte, S. Choe, M. Perán, J.A. Marchal, Activin A/BMP2 chimera AB235
26
27
454 drives efficient redifferentiation of long term cultured autologous chondrocytes, Sci. Rep. 5
28
29
455 (2015) 16400.
31
32
456 [4] M. Schnabel, S. Marlovits, G. Eckhoff, I. Fichtel, L. Gotzen, V. Vécsei, J. Schlegel,
33
34
457 Dedifferentiation-associated changes in morphology and gene expression in primary human
36
37
458 articular chondrocytes in cell culture, Osteoarthr. Cartil. 10 (2002) 62–70.
38
39
459 [5] C.B. Foldager, A.B. Nielsen, S. Munir, M. Ulrich-Vinther, K. Søballe, C. Bünger, M. Lind,
41
42
460 Combined 3D and hypoxic culture improves cartilage-specific gene expression in human
43
44
461 chondrocytes., Acta Orthop. 82 (2011) 234–240.
46
47
462 [6] T. Takahashi, T. Ogasawara, Y. Asawa, Y. Mori, E. Uchinuma, T. Takato, K. Hoshi, Three-
48
49
463 dimensional microenvironments retain chondrocyte phenotypes during proliferation culture.,
51
52
464 Tissue Eng. 13 (2007) 1583–1592.
53
54
465 [7] E.A. Makris, A.H. Gomoll, K.N. Malizos, J.C. Hu, K.A. Athanasiou, Repair and tissue
55
56
466 engineering techniques for articular cartilage, Nat. Rev. Rheumatol. 11 (2014) 21–34.
58
59
467 [8] W. Bartlett, J.A. Skinner, C.R. Gooding, R.W.J. Carrington, A.M. Flanagan, T.W.R. Briggs,
60

61
62
63
64
65

- 468 G. Bentley, Autologous chondrocyte implantation versus matrix-induced autologous
469 chondrocyte implantation for osteochondral defects of the knee: a prospective, randomised
2 study., *J. Bone Joint Surg. Br.* 87 (2005) 640–645.
3
470
4
5
471 [9] F. Zeifang, D. Oberle, C. Nierhoff, W. Richter, B. Moradi, H. Schmitt, Autologous
7
472 chondrocyte implantation using the original periosteum-cover technique versus matrix-
8
9 associated autologous chondrocyte implantation: a randomized clinical trial., *Am. J. Sports*
10
11
12
13
14
1474
14
15
1475 [10] D.W. Hutmacher, Scaffolds in tissue engineering bone and cartilage., *Biomaterials.* 21
16
17
1476 (2000) 2529–2543.
18
19
20
1477 [11] S.B. Cohen, C.M. Meirisch, H.A. Wilson, D.R. Diduch, The use of absorbable co-polymer
21
22
23
24
25
2478
24
25
2479
26
27
2480 [12] S.C. Skaalure, S.O. Dimson, A.M. Pennington, S.J. Bryant, Semi-interpenetrating networks
28
29
30
31
32
33
34
3481
31
32
33
3482
34
35
36
3483 [13] W.R. Coury AJ, Levy RJ, Ratner BD, Shoen FJ, Williams DF, Degradation of materials in
37
38
39
40
41
42
43
3484
38
39
40
41
42
43
44
4485
41
42
43
4486 [14] L. Glennon-Alty, R. Williams, S. Dixon, P. Murray, Induction of mesenchymal stem cell
45
46
47
48
49
50
51
487
46
47
48
49
50
51
52
53
54
5488
48
49
50
51
52
53
54
55
56
57
58
59
5489
51
52
53
54
55
56
57
58
59
60
61
62
63
64
65
- [15] M. Sancho-Tello, F. Forriol, J.J.M. de Llano, C. Antolinos-Turpin, J.A. Gómez-Tejedor, J.L.G. Ribelles, C. Carda, Biostable Scaffolds of Polyacrylate Polymers Implanted in the Articular Cartilage Induce Hyaline-Like Cartilage Regeneration in Rabbits, *Int. J. Artif. Organs.* 40 (2017) 350–357.
- [16] M.-C. Tsai, K.-C. Hung, S.-C. Hung, S. Hsu, Evaluation of biodegradable elastic scaffolds made of anionic polyurethane for cartilage tissue engineering., *Colloids Surf. B.*

- 494 Biointerfaces. 125 (2015) 34–44.
- 495 [17] D. Seliktar, Designing cell-compatible hydrogels for biomedical applications., Science. 336
2
3
496 (2012) 1124–1128.
4
5
- 497 [18] Y. Li, J. Rodrigues, H. Tomás, Injectable and biodegradable hydrogels: gelation,
7
498 biodegradation and biomedical applications., Chem. Soc. Rev. 41 (2012) 2193–2221.
9
- 10
499 [19] F. Khan, R.S. Tare, J.M. Kanczler, R.O.C. Oreffo, M. Bradley, Strategies for cell
11
12
13
14
1500 manipulation and skeletal tissue engineering using high-throughput polymer blend
14
15
1501 formulation and microarray techniques., Biomaterials. 31 (2010) 2216–2228.
16
17
- 1802 [20] M.S. Algahtani, D.J. Scurr, A.L. Hook, D.G. Anderson, R.S. Langer, J.C. Burley, M.R.
19
20
2103 Alexander, M.C. Davies, High throughput screening for biomaterials discovery., J. Control.
21
22
2304 Release. 190 (2014) 115–126.
24
- 25
2605 [21] A.L. Hook, D.G. Anderson, R. Langer, P. Williams, M.C. Davies, M.R. Alexander, High
26
27
2806 throughput methods applied in biomaterial development and discovery., Biomaterials. 31
29
30
3107 (2010) 187–198.
31
32
- 3308 [22] J.-F. Thaburet, H. Mizomoto, M. Bradley, High-Throughput Evaluation of the Wettability of
34
35
3609 Polymer Libraries, Macromol. Rapid Commun. 25 (2004) 366–370.
36
37
- 380 [23] S. Pernagallo, J.J. Diaz-Mochon, Polymer Microarrays for Cellular High-Content Screening,
38
39
4011 in: Methods Mol. Biol., 2011: pp. 171–180.
41
- 42
43012 [24] E. López-Ruiz, M. Perán, J. Cobo-Molinos, G. Jiménez, M. Picón, M. Bustamante, F.
44
45
4613 Arrebola, M.C. Hernández-Lamas, A.D. Delgado-Martínez, E. Montañez, J.A. Marchal,
46
47
4814 Chondrocytes extract from patients with osteoarthritis induces chondrogenesis in
48
49
5015 infrapatellar fat pad-derived stem cells, Osteoarthr. Cartil. 21 (2013) 246–258.
51
- 52
53016 [25] C. Duffy, A. Venturato, A. Callanan, A. Lilienkampf, M. Bradley, Arrays of 3D double-
53
54
5517 network hydrogels for the high-throughput discovery of materials with enhanced physical
56
57
5818 and biological properties., Acta Biomater. 34 (2016) 104–112.
58
- 59
6019 [26] S. Yashiki, R. Umegaki, M. Kino-Oka, M. Taya, Evaluation of attachment and growth of
61
62
63
64
65

- 520 anchorage-dependent cells on culture surfaces with type I collagen coating., *J. Biosci.*
521 *Bioeng.* 92 (2001) 385–388.
- 522 [27] S.-J. Chen, C.-C. Lin, W.-C. Tuan, C.-S. Tseng, R.-N. Huang, Effect of recombinant
523 galectin-1 on the growth of immortal rat chondrocyte on chitosan-coated PLGA scaffold., *J.*
524 *Biomed. Mater. Res. A.* 93 (2010) 1482–1492.
- 525 [28] S. Martinez-Diaz, N. Garcia-Giralt, M. Lebourg, J.-A. Gómez-Tejedor, G. Vila, E. Caceres,
526 P. Benito, M.M. Pradas, X. Nogues, J.L.G. Ribelles, J.C. Monllau, In vivo evaluation of 3-
527 dimensional polycaprolactone scaffolds for cartilage repair in rabbits., *Am. J. Sports Med.* 38
528 (2010) 509–519.
- 529 [29] M. Lebourg, J.R. Rochina, T. Sousa, J. Mano, J.L.G. Ribelles, Different hyaluronic acid
530 morphology modulates primary articular chondrocyte behavior in hyaluronic acid-coated
531 polycaprolactone scaffolds., *J. Biomed. Mater. Res. A.* 101 (2013) 518–527.
- 532 [30] H. Tamagawa, S. Popovic, M. Taya, Pores and diffusion characteristics of porous gels,
533 *Polymer (Guildf).* 41 (2000) 7201–7207.
- 534 [31] C. Chung, J.A. Burdick, Engineering cartilage tissue, *Adv. Drug Deliv. Rev.* 60 (2008) 243–
535 262.
- 536 [32] S. Gerecht, S.A. Townsend, H. Pressler, H. Zhu, C.L.E. Nijst, J.P. Bruggeman, J.W. Nichol,
537 R. Langer, A porous photocurable elastomer for cell encapsulation and culture, *Biomaterials.*
538 28 (2007) 4826–4835.
- 539 [33] S. Yu, F.L. Ng, K.C.C. Ma, F.L. Ng, J. Zhao, S.K.K. Tong, Development of porous polymer
540 monolith by photoinitiated polymerization, *J. Appl. Polym. Sci.* 120 (2011) 3190–3195.
- 541 [34] N.A. Peppas, J.Z. Hilt, A. Khademhosseini, R. Langer, *Hydrogels in Biology and Medicine:*
542 *From Molecular Principles to Bionanotechnology,* *Adv. Mater.* 18 (2006) 1345–1360.
- 543 [35] S. Columbus, L.K. Krishnan, V. Kalliyana Krishnan, Relating pore size variation of poly (ϵ -
544 caprolactone) scaffolds to molecular weight of porogen and evaluation of scaffold properties
545 after degradation, *J. Biomed. Mater. Res. Part B Appl. Biomater.* 102 (2014) 789–796.

- 546 [36] A.G. Lee, C.P. Arena, D.J. Beebe, S.P. Palecek, Development of macroporous poly(ethylene
547 glycol) hydrogel arrays within microfluidic channels., *Biomacromolecules*. 11 (2010) 3316–
548 3324.
549 [37] O. Okay, Macroporous copolymer networks, n.d.
550 <https://web.itu.edu.tr/okayo/pdf/00review.pdf> (accessed January 22, 2019).
551 [38] N. Annabi, J.W. Nichol, X. Zhong, C. Ji, S. Koshy, A. Khademhosseini, F. Dehghani,
552 Controlling the porosity and microarchitecture of hydrogels for tissue engineering., *Tissue*
553 *Eng. Part B. Rev.* 16 (2010) 371–383.
554 [39] A.M. Bhosale, J.B. Richardson, Articular cartilage: structure, injuries and review of
555 management, *Br. Med. Bull.* 87 (2008) 77–95.
556 [40] S. Marlovits, M. Hombauer, M. Truppe, V. Vècsei, W. Schlegel, Changes in the ratio of
557 type-I and type-II collagen expression during monolayer culture of human chondrocytes., *J.*
558 *Bone Joint Surg. Br.* 86 (2004) 286–295.
559 [41] S. Yang, K.F. Leong, Z. Du, C.K. Chua, The design of scaffolds for use in tissue
560 engineering. Part I. Traditional factors., *Tissue Eng.* 7 (2001) 679–689.
561 [42] J. Zeltinger, J.K. Sherwood, D.A. Graham, R. Müller, L.G. Griffith, Effect of pore size and
562 void fraction on cellular adhesion, proliferation, and matrix deposition., *Tissue Eng.* 7 (2001)
563 557–572.
564 [43] J.K. Sherwood, S.L. Riley, R. Palazzolo, S.C. Brown, D.C. Monkhouse, M. Coates, L.G.
565 Griffith, L.K. Landeen, A. Ratcliffe, A three-dimensional osteochondral composite scaffold
566 for articular cartilage repair., *Biomaterials*. 23 (2002) 4739–4751.
567 [44] S. Nehrer, H.A. Breinan, A. Ramappa, G. Young, S. Shortkroff, L.K. Louie, C.B. Sledge, I.
568 V Yannas, M. Spector, Matrix collagen type and pore size influence behaviour of seeded
569 canine chondrocytes., *Biomaterials*. 18 (1997) 769–776.
570 [45] H. Stenhamre, U. Nannmark, A. Lindahl, P. Gatenholm, M. Brittberg, Influence of pore size
571 on the redifferentiation potential of human articular chondrocytes in poly(urethane urea)

- 572 scaffolds., *J. Tissue Eng. Regen. Med.* 5 (2011) 578–588.
- 573 [46] F. Dell’Accio, C. De Bari, F.P. Luyten, Molecular markers predictive of the capacity of
2 expanded human articular chondrocytes to form stable cartilage in vivo., *Arthritis Rheum.* 44
3
574 (2001) 1608–1619.
4
5
575
- 576 [47] S. Lee, D.S. Yoon, S. Paik, K.-M. Lee, Y. Jang, J.W. Lee, microRNA-495 inhibits
6
7
8
9
10
577 chondrogenic differentiation in human mesenchymal stem cells by targeting Sox9., *Stem*
11
12
13
14
578 *Cells Dev.* 23 (2014) 1798–1808.
- 15
579 [48] J. Liao, N. Hu, N. Zhou, L. Lin, C. Zhao, S. Yi, T. Fan, W. Bao, X. Liang, H. Chen, W. Xu,
16
17
18
19
20
580 C. Chen, Q. Cheng, Y. Zeng, W. Si, Z. Yang, W. Huang, Sox9 potentiates BMP2-induced
21
22
23
24
581 chondrogenic differentiation and inhibits BMP2-induced osteogenic differentiation., *PLoS*
25
26
27
28
29
582 *One.* 9 (2014) e89025.
- 30
583 [49] A. Barlic, M. Drobnic, E. Malicev, N. Kregar-Velikonja, Quantitative analysis of gene
31
32
33
34
35
584 expression in human articular chondrocytes assigned for autologous implantation., *J. Orthop.*
36
37
38
39
585 *Res.* 26 (2008) 847–853.
- 40
586 [50] M. Brittberg, A. Lindahl, A. Nilsson, C. Ohlsson, O. Isaksson, L. Peterson, Treatment of
41
42
43
44
45
587 Deep Cartilage Defects in the Knee with Autologous Chondrocyte Transplantation, *N. Engl.*
46
47
48
49
50
588 *J. Med.* 331 (1994) 889–895.
- 51
589 [51] H.J. Kim, S.R. Park, H.J. Park, B.H. Choi, B.-H. Min, Potential predictive markers for
52
53
54
55
56
590 proliferative capacity of cultured human articular chondrocytes: PCNA and p21., *Artif.*
57
58
59
60
61
591 *Organs.* 29 (2005) 393–398.
- 62
592 [52] J. Walser, K.S. Stok, M.D. Caversaccio, S.J. Ferguson, Direct electrospinning of 3D auricle-
63
64
65
66
67
593 shaped scaffolds for tissue engineering applications., *Biofabrication.* 8 (2016) 25007.
- 68
594 [53] V.P. Ribeiro, A. da Silva Morais, F.R. Maia, R.F. Canadas, J.B. Costa, A.L. Oliveira, J.M.
69
70
71
72
73
595 Oliveira, R.L. Reis, Combinatory approach for developing silk fibroin scaffolds for cartilage
74
75
76
77
78
596 regeneration., *Acta Biomater.* 72 (2018) 167–181.
- 79
597 [54] A.S. Sumayya, G. Muraleedhara Kurup, Biocompatibility of subcutaneously implanted
80
81
82
83
84
85

598 marine macromolecules cross-linked bio-composite scaffold for cartilage tissue engineering
599 applications, *J. Biomater. Sci. Polym. Ed.* 29 (2018) 257–276.
2
3
600 [55] J. Zwingmann, A.T. Mehlhorn, N. Südkamp, B. Stark, M. Dauner, H. Schmal, Chondrogenic
4
5
601 Differentiation of Human Articular Chondrocytes Differs in Biodegradable PGA/PLA
7
8
602 Scaffolds, *Tissue Eng.* 13 (2007) 2335–2343.
9

10
603
11
12
604
13
14
15
605
16
17
606
18
19
20
607
21
22
608
23
24
25
609
26
27
610
28
29
611
30
31
32
612
33
34
613
35
36
37
614
38
39
615
40
41
42
616
43
44
617
45
46
47
618
48
49
619
50
51
620
52
53
54
621
55
56
622
57
58
59
623
60
61
62
63
64
65

624 **Figure legends**

625 **Figure 1. Cell viability and chondrogenic markers expression after 21 days of chondrocyte**
2
3
626 **culture on hydrogels. (a)** Representative confocal laser scanning microscope images of primary
4
5
627 human chondrocytes cultured in 3D hydrogels for 21 days. Live cells show green fluorescence
7
8
628 (CTG) and dead cells are labeled with propidium iodide (PI) in red. Scale bar = 100 μm . **(b)**
9
10
629 Cartilage matrix-related markers Col 2 (red) and Col 1 (green) staining of primary human
11
12
630 chondrocytes cultured on the hydrogels for 21 days. Scale bar = 100 μm . **(c)** Histological staining of
13
14
631 hydrogels sections by Hematoxylin-Eosin (H&E), Masson's Trichrome (MT) and Alcian Blue (AB)
15
16
632 staining. Magnification 20x. Scale bar = 100 μm .

20
21
22
633
23
634 **Figure 2. Structural and mechanical properties of both lyophilised and non-lyophilised**
24
25
635 **PA204-2 hydrogels. (a)** Chemical structure of PA204-2. **(b)** Representative images of PA204-2
26
27
636 hydrogels before cells were seeded. **(c)** Environmental scanning electron microscopy (ESEM)
28
29
637 images of both lyophilised and non-lyophilised PA204-2 hydrogels structure. **(d and e)** 2-D image
30
31
638 (Scale bar = 1 mm) and quantitative analysis of the hydrogel's microstructure determined by micro-
32
33
639 CT. **(f)** Mechanical testing of the hydrogels.

34
35
36
37
38
39
640
40
641 **Figure 3. Analysis of chondrocyte phenotype of PA204-2 hydrogels after 21 days. (a)** ESEM
41
42
642 images of chondrocytes cultured on hydrogels. **(b)** Real-time quantitative PCR analysis of
43
44
643 chondrogenic markers. All gene expressions were normalized with values of chondrocytes cultured
45
46
644 for 21 days in standard culture medium (CTL). Chondrocytes cultured in a pellet system for 21 days
47
48
645 were used as a 3D culture system control. Statistical significant differences were found (* $p < 0.05$,
49
50
646 ** $p < 0.01$) as compared to gene expressions between CTL and PA204-2, and when compared
51
52
647 PA204-2 and Pellet (# $p < 0.05$, ## $p < 0.01$). **(c)** Measurement of GAGs content of primary human
53
54
648 chondrocytes normalized by DNA content. Significant differences were found when compared 1
55
56
649 and 3 weeks (** $p < 0.01$), and when compared PA204-2 L and PA204-2 UL hydrogels (## $p < 0.01$).

650 (d) Metabolic activity/proliferation of chondrocytes examined by Alamar blue assay. PA204-2 L
651 (PA204-2 lyophilised), PA204-2 NL (PA204-2 non-lyophilised).

2
3
652 4
5
653 **Figure 4. *In vivo* biocompatibility of PA204-2 hydrogels.** (a) Representative images of hydrogels
7
854 after implantation into immunocompetent CD-1 mice, and integration into surrounding tissue after 3
9
10 weeks of *in vivo* assay. (b) Confocal laser scanning microscope images of hydrogels harvested from
11
12 mice and stained with CTG (green) and IP (red). Magnification 20x. Scale bar = 100 µm. (c)
1356
14
15
1657
16
17
1858
19
20
2159
21
22
23
24

25
2651
26
27
2852
29
30
3153
31
32
3354
34
3555
36
37
3856
38
39
4057
41
42
4358
43
44
4559
46
47
4860
48
49
5061
51
52
53
54
5562
56
57
58
59
60
61
62
63
64
65

65
66
67
68
69
70
71
72
73
74
75
76
77
78
79
80
81
82
83
84
85
86
87
88
89
90
91
92
93
94
95
96
97
98
99
100

677 **Table 1.** Monomers composition of 'hit' polymers

| Polymer | Monomer (1) | Monomer (2) | Monomer (3) | M (1) | M (2) | M (3) |
|---------|-------------|-------------|-------------|-------|-------|-------|
| PA167 | HEMA | BAEMA | - | 50 | 50 | - |
| PA204 | MMA | MA-H | - | 90 | 10 | - |
| PA234 | MMA | MA-H | DEAEMA | 70 | 20 | 10 |
| PA391 | EMA | DEAEMA | - | 70 | 30 | - |
| PA202 | MMA | AES-H | - | 70 | 30 | - |
| PA410 | BMA | DEAEA | - | 50 | 50 | - |
| PA309 | MMA | GMA | DnHA | 90 | 10 | - |
| PA520 | MEMA | DEAEMA | St | 60 | 30 | 10 |
| PA460 | MEMA | DEAEA | THFFMA | 60 | 30 | 10 |

| | Diol | DIS | Extender | ratio (mol) | | |
|-------|---------------|-----|----------|-------------|-------------|----------|
| | | | | monomer (1) | monomer (2) | Extender |
| PU153 | PTMG (250 Da) | HDI | PG | 23 | 52 | 23 |

678 HEMA: 2-hydroxyethylmethacrylate; BAEMA: 2-(tert-butylamino)ethyl methacrylate; MMA:
679 Methyl methacrylate; MA-H: Methacrylic acid; EMA: ethyl methacrylate; DEAEMA: 2-
680 (diethylamino)ethyl methacrylate; AES-H: mono-2-(acryloyoxy)ethyl succinate; BMA: butyl
681 methacrylate; DEAEA: 2-(diethylamino)ethyl acrylate; GMA glycidyl methacrylate; DnHA di-n-
682 hexylamine; MEMA: 2-methoxyethylmethacrylate; THFFMA: tetrahydrofurfuryl methacrylate; St:
683 styrene.

685 **Table 2.** Composition of polymerisation solutions used to prepare PA204 gels

| | 204-2 | 204-2A |
|---------------------|-------|--------|
| Monomer mix (PA204) | 10.0% | 10.0% |
| PEGDA700 | 2.0% | 2.0% |
| PEG (porogen) | 2.0% | 4.0% |
| APS | 0.5% | 0.5% |
| TEMED | 2.0% | 2.0% |
| Water | 20.0% | 30.0% |
| NMP | 63.5% | 51.5% |

687 PA204 monomer mix: MMA (Methyl methacrylate) and MA-H (Methacrylic acid)

| Constituent | Composition (μ L) | |
|---------------------------------|------------------------|--------|
| | 204-2 | 204-2A |
| TEMED solution (10% w/w in NMP) | 500 | 500 |

1
2
3
4
5
6
7
8
9
10
11
12
13
14
15
16
17
18
19
20
21
22
23
24
25
26
27
28
29
30
31
32
33
34
35
36
37
38
39
40
41
42
43
44
45
46
47
48
49
50
51
52
53
54
55
56
57
58
59
60
61
62
63
64
65

| | | |
|--|-----|-----|
| Monomer solution (391 or 204) (50% w/w in NMP) | 500 | 500 |
| PEGDA700 solution (10% w/w in NMP) | 500 | 500 |
| APS solution (2.5% w/w)* | 500 | 500 |
| PEG solution (20% w/w in water) | 250 | 500 |
| NMP | 250 | 0 |

* APS solution was prepared in 50% NMP (w/w in water)

Figure 1
[Click here to download high resolution image](#)

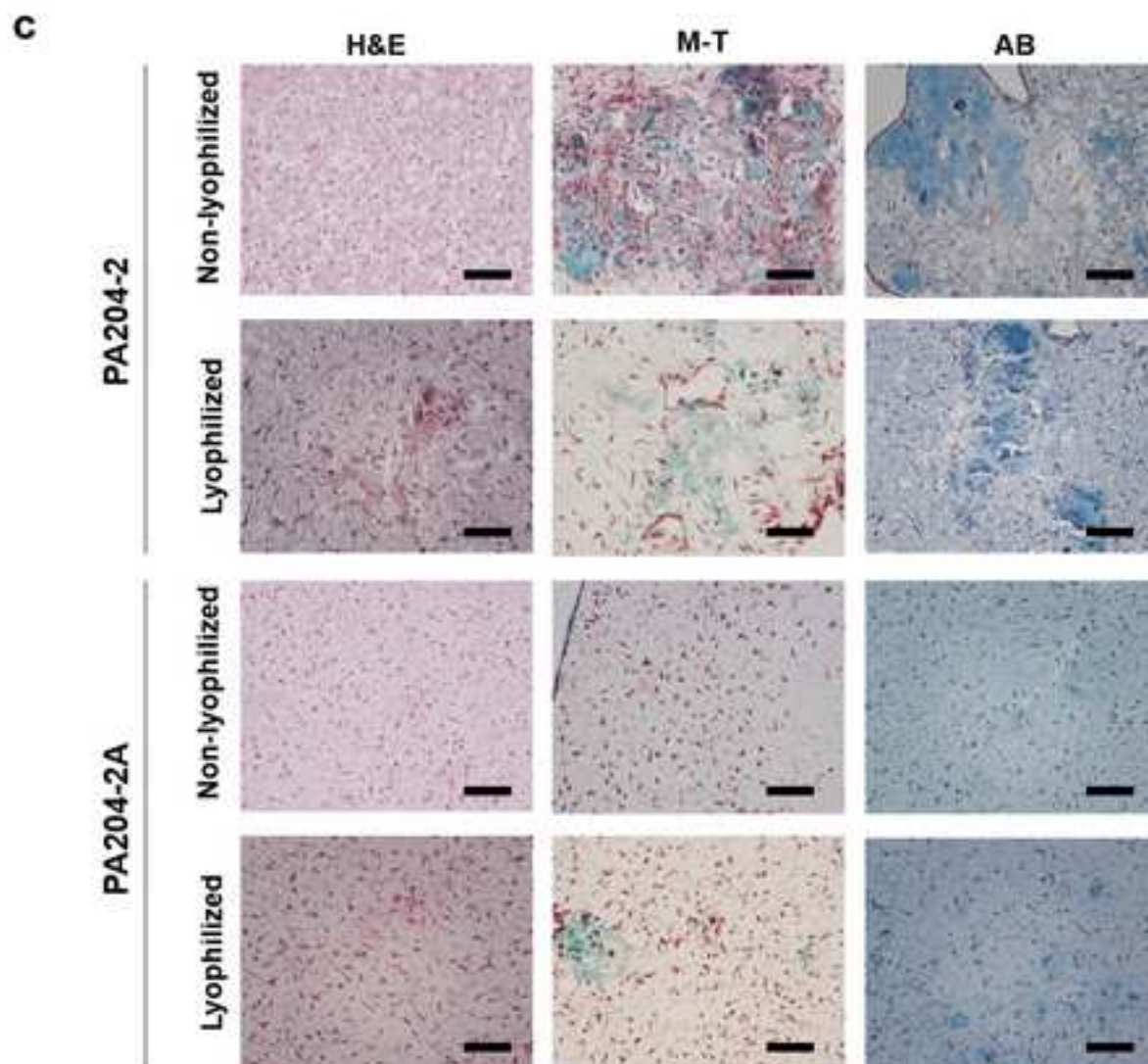
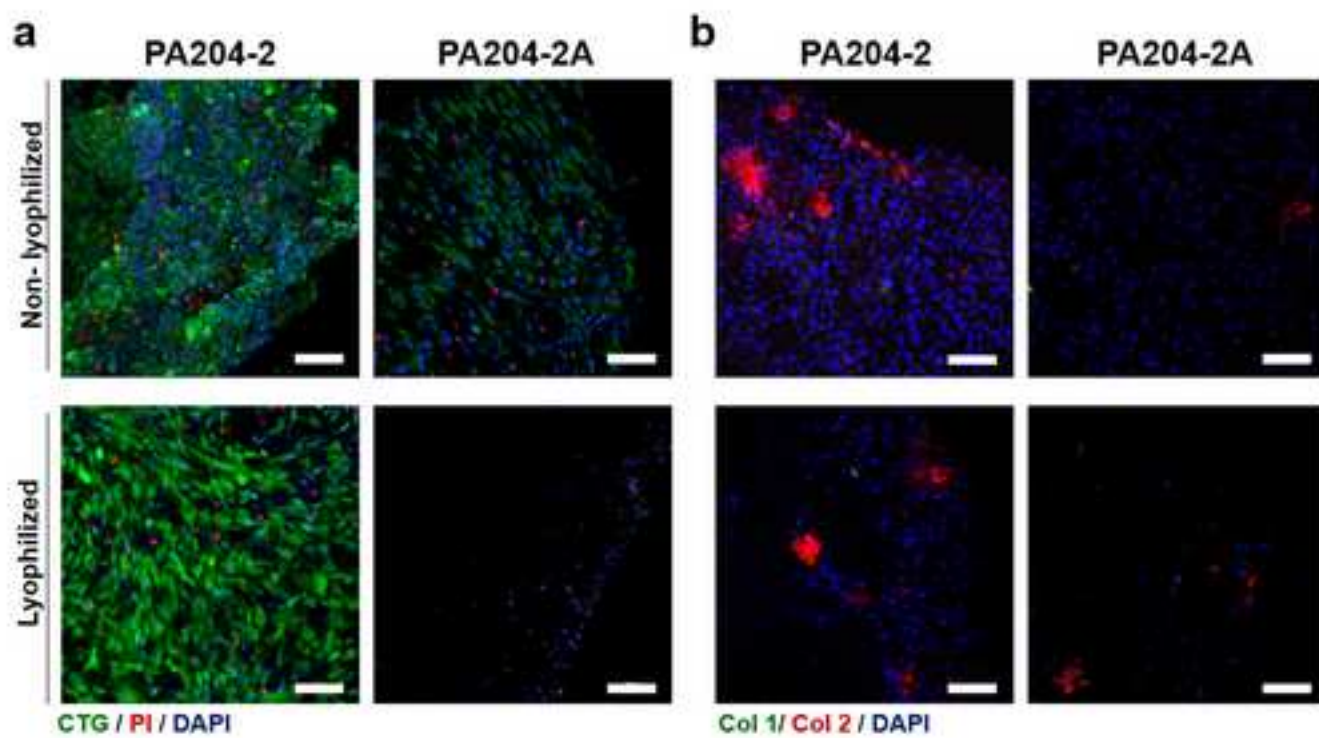


Figure 2

[Click here to download high resolution image](#)

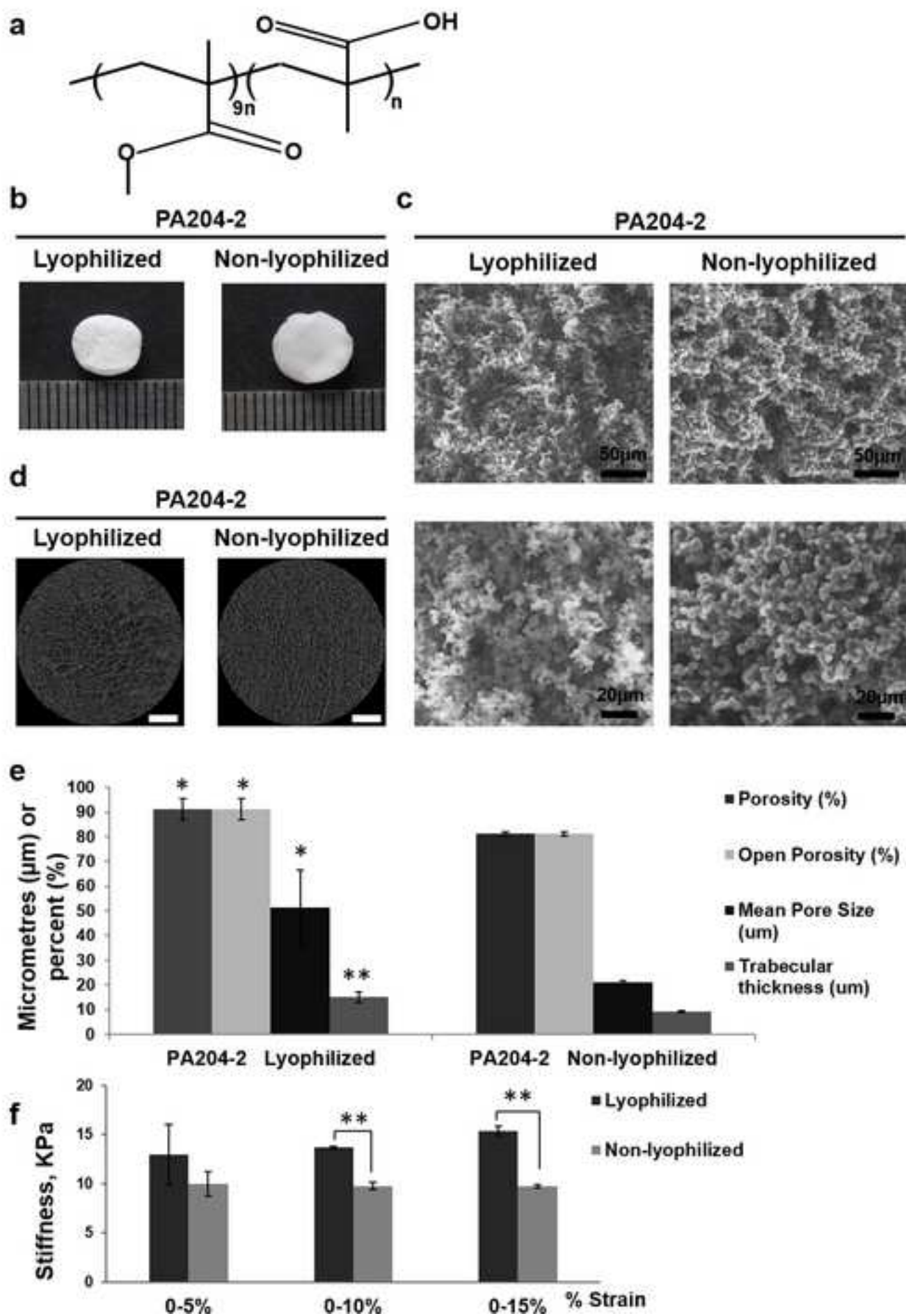


Figure 3
[Click here to download high resolution image](#)

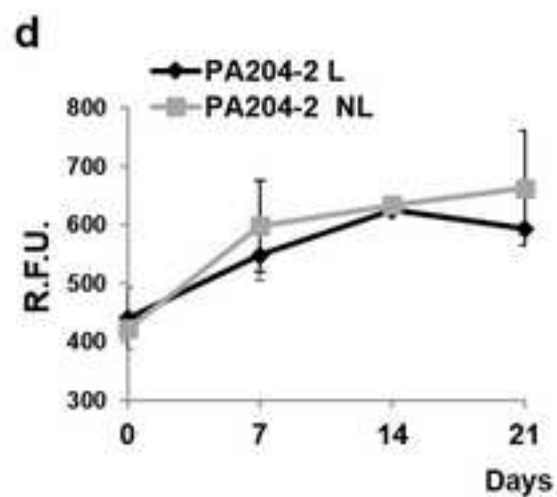
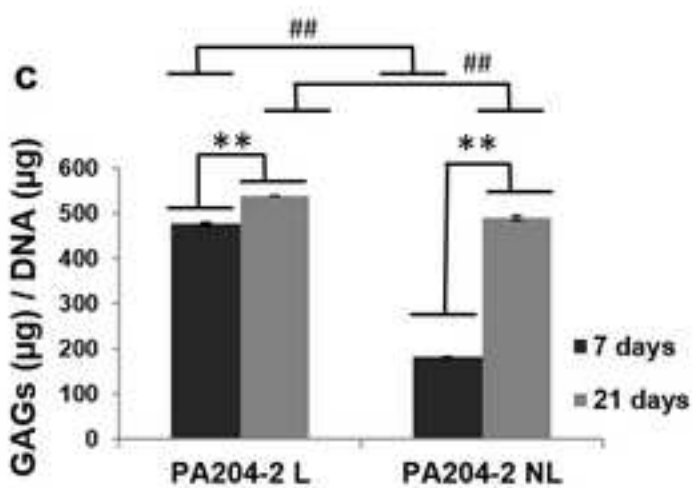
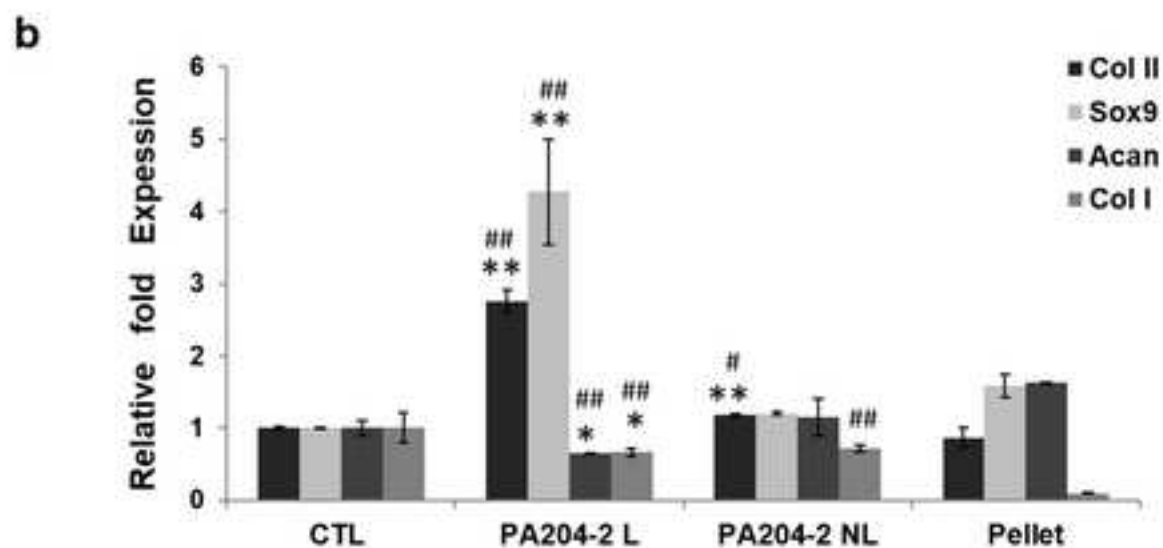
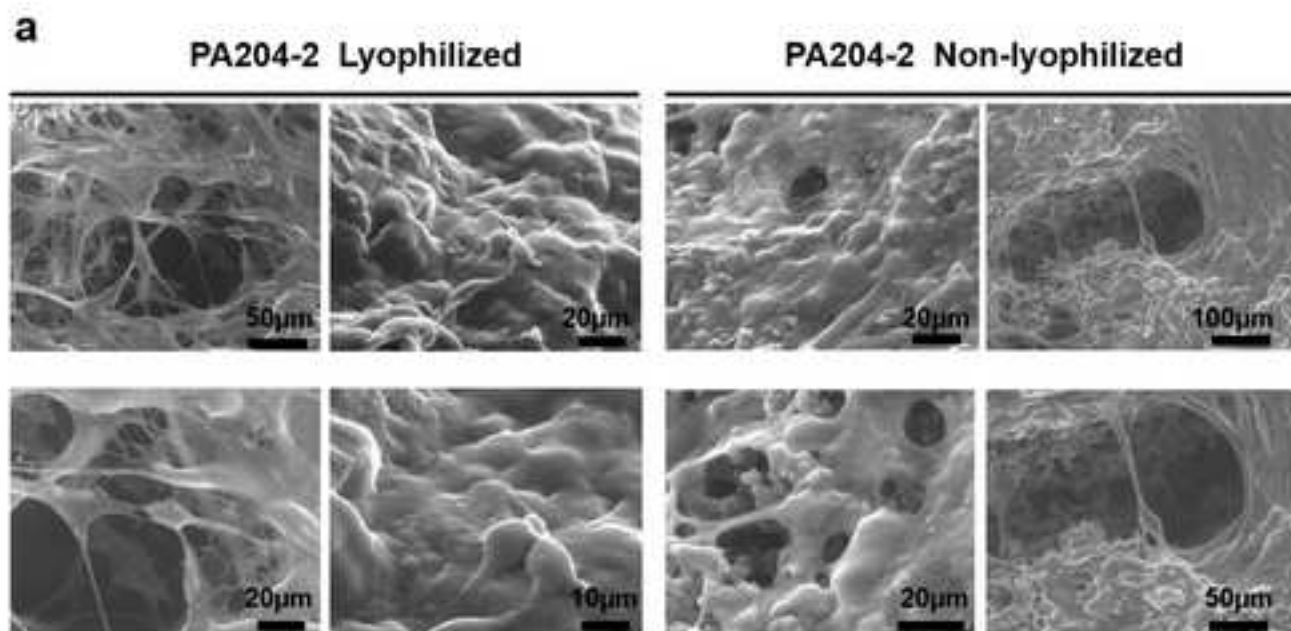


Figure 4
[Click here to download high resolution image](#)

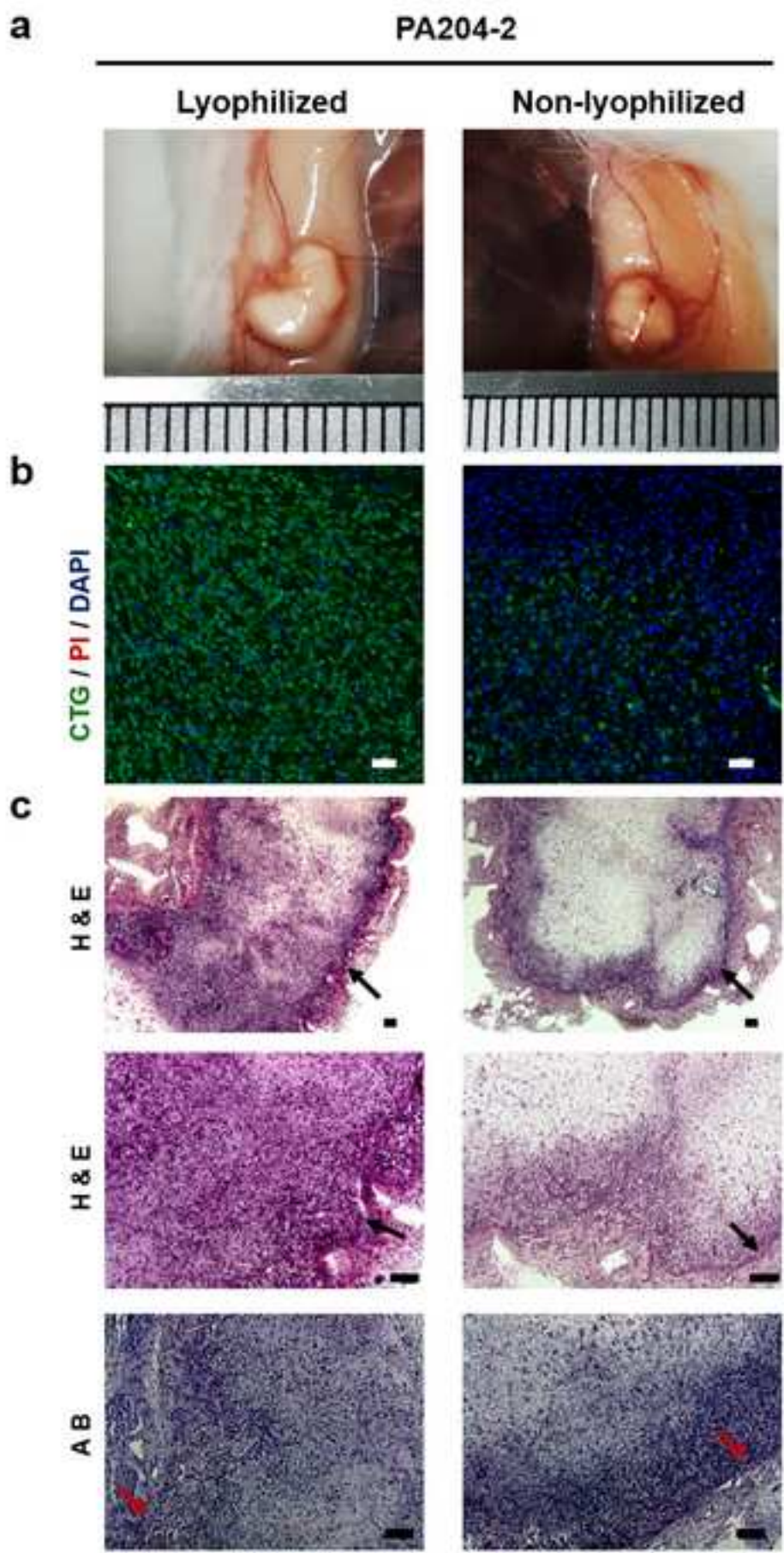
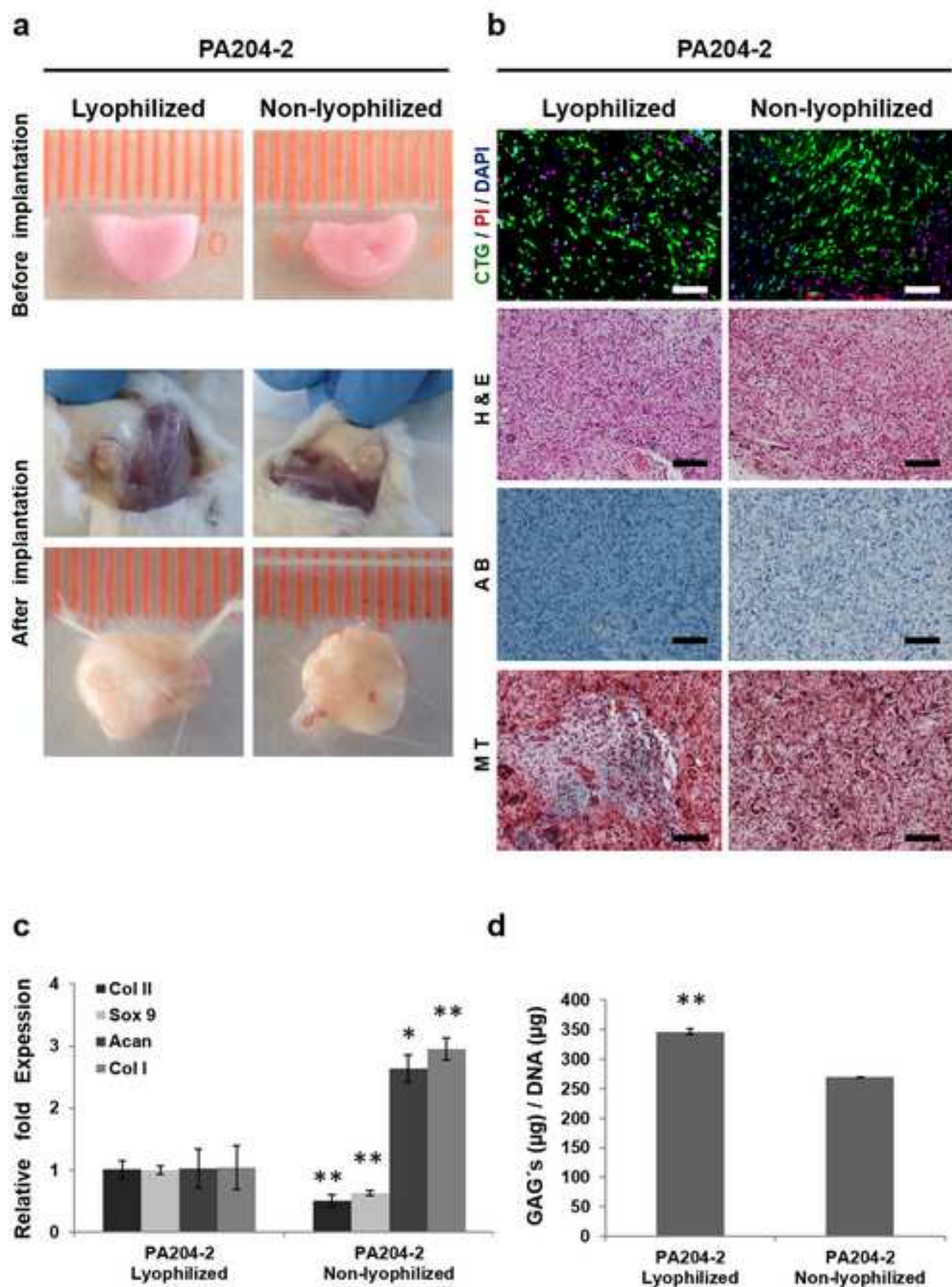


Figure 5
[Click here to download high resolution image](#)



Supplementary Material

[Click here to download Supplementary Material: Jimnez et al_Supplementary data.doc](#)